2, 287-303.
Weiner, S. J., Kollman, P. A., Case, D., Singh, U. C., Ghio, C., Alagona, G., Profeta, S., Jr., & Weiner, P. K. (1984) J. Am. Chem. Soc. 106, 765-784.
Zakrzewska, K., & Pullman, B. (1986) J. Biomol. Struct. Dyn. 4, 127-136.

pH-Induced Denaturation of Proteins: A Single Salt Bridge Contributes 3-5 kcal/mol to the Free Energy of Folding of T4 Lysozyme

D. Eric Anderson, Wayne J. Becktel, and F. W. Dahlquist*
Institute of Molecular Biology and Department of Chemistry, University of Oregon, Eugene, Oregon 97403
Received August 29, 1989; Revised Manuscript Received November 1, 1989

ABSTRACT: The energetics of a salt bridge formed between the side chains of aspartic acid 70 (Asp70) and histidine 31 (His31) of T4 lysozyme have been examined by nuclear magnetic resonance techniques. The pK_a values of the residues in the native state are perturbed from their values in the unfolded protein such that His31 has a pK_a value of 9.1 in the native state and 6.8 in the unfolded state at 10 °C in moderate salt. Similarly, the aspartate pK_a is shifted to a value of about 0.5 in the native state from its value of 3.5-4.0 in the unfolded state. These shifts in pK_a show that the salt bridge is stabilized 3-5 kcal/mol. This implies that the salt bridge stabilizes the native state by 3-5 kcal/mol as compared to the unfolded state. This is reflected in the thermodynamic stability of mutants of the protein in which Asp70, His31, or both are replaced by asparagine. These observations and consideration of the thermodynamic coupling of protonation state to folding of proteins suggest a mechanism of acid denaturation in which the unfolded state is progressively stabilized by protonation of its acid residues as pH is lowered below pH 4. The unfolded state is stabilized only if acidic groups in the folded state have lower pK_a values than in the unfolded state. When the pH is sufficiently low, the acid groups of both the native and unfolded states are fully protonated, and the apparent unfolding equilibrium constant becomes pH independent. Similar arguments apply to base-induced unfolding. These observations suggest that the electrostatic contribution of each ionizable group to the stability of the folded state can be directly assessed by simply measuring its apparent pK_a by NMR or other methods.

The pH dependence of the thermodynamic stability of proteins has long been of interest to biochemists. Linderström-Lang (1924) was one of the first to suggest a plausible reason for the lowered stability of proteins at extremes of pH. In this view, the stability was determined by electrostatic interactions in the native, folded state of a protein. For example, at acidic pH, the decreased stability would be the result of unfavorable electrostatic interactions introduced by the increase in positive charge on a protein. Similar arguments accounted for the decrease in stability observed in highly basic solutions due to repulsion of negative charges. The theory predicted maximum stability at or near the isoelectric point of the protein where the net charge is zero. This model has been extended to include more detailed considerations of charge–charge interactions of the native state (Matthews & Gurd, 1986).

A number of proteins, with acidic or basic isoelectric points, are observed to have maximal thermodynamic stability near neutrality. This observation suggests that considerations in addition to overall charge are important in determining the contribution of ionizable groups to the overall folding energy of globular proteins. For example, the lysozyme produced by the bacteriophage T4 is a rather basic protein with an isoelectric point above pH 10 yet is most stable near pH 5. This genetically manipulable, 164-residue protein without disulfide bonds has been the object of intense structural [Matthews & Remington, 1974; Matsumura et al. (1988) and Nicholson et al. (1988) and references cited therein], thermodynamic (Hawkes et al., 1984; Becktel & Baase, 1987; Becktel & Schellman, 1987), and spectroscopic (McIntosh et al., 1987a,b) investigation and provides an excellent model protein in which to study interactions between ionizable residues and protein stability.

Materials and Methods

Site-directed mutagenesis (Zoeller & Smith, 1983) was performed essentially as described by Kunkel (1985) on M13 single-strand DNA containing a derivative of the T4 lysozyme gene in which codons for cysteine residues 54 and 97 had been changed to encode threonine and alanine, respectively [Matsumara et al. (1988) and references cited therein]. Directed mutations were H31N, D70E, D70N, and H31N/D70N. Mutations were confirmed by chain-termination dideoxy sequencing (Sanger et al., 1977). T4 lysozyme was produced and specifically enriched in [4-^{13}C]aspartic acid (99%, Merck Sharp & Dohme of Canada) according to an approach described elsewhere (Muchmore et al., 1989). Reversible unfolding of T4 lysozymes was monitored with the change in dichroism at 223 nm, as has been described (Elwell & Schellman, 1977; Becktel & Baase, 1987).

For histidine titrations of the folded state, the protein was transferred to a D_2O buffer of 10 mM D_3PO_4 and 10 mM KCl, heated to 55 °C for 0.5 h, and slowly cooled. This treatment reversibly unfolds the protein and allows rapid exchange of all amide protons by deuterons. After refolding, the protein retains its enzymatic activity and appears to be otherwise identical with the native protein before exchange.

All titrations and pH measurements were performed at 10 °C. Proton NMR measurements of the pH dependence of

* To whom correspondence should be addressed.

0006-2960/90/0429-2403$02.50/0

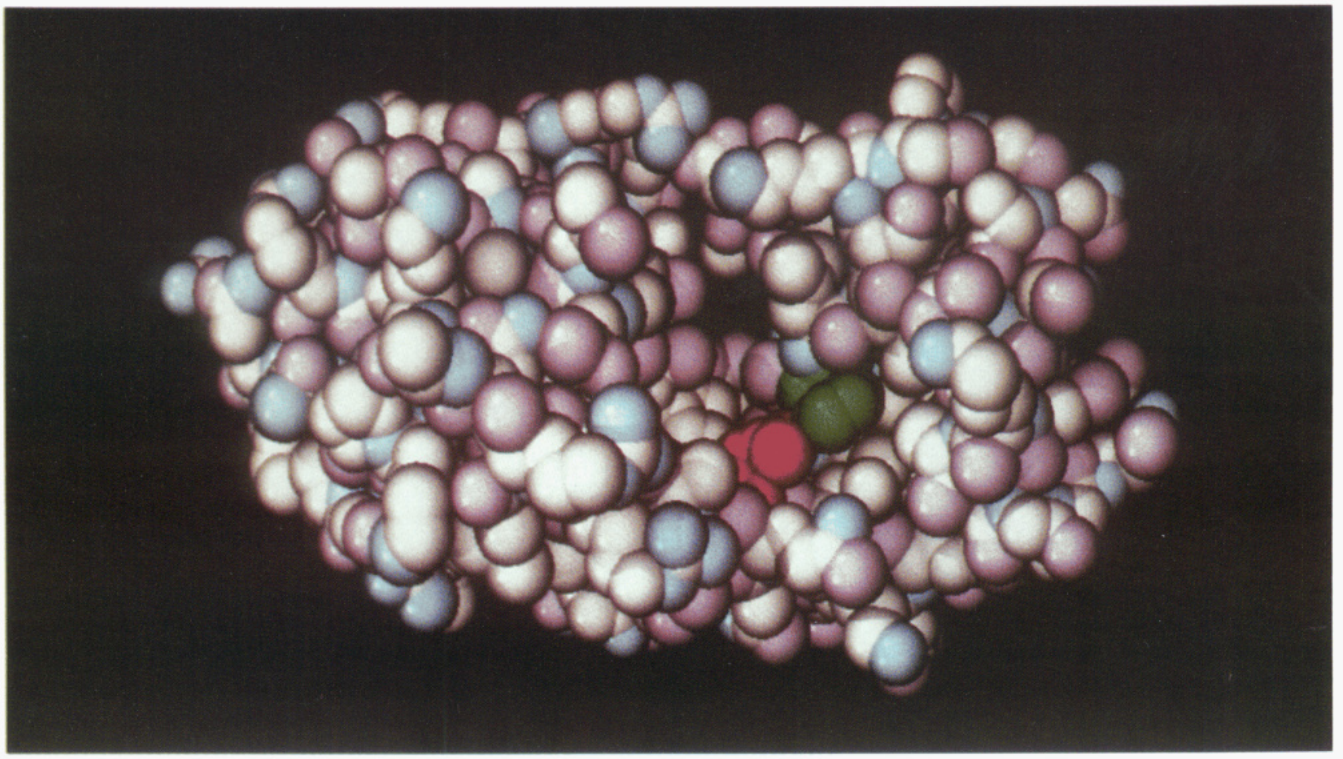

FIGURE 1: Computer-generated CPK model of T4 lysozyme using the C, N, and O atomic coordinates derived by X-ray crystallography. The red atoms indicate Asp70, and the green atoms indicate His31. The light blue atoms are nitrogen, purple atoms are oxygen, and white atoms are carbon of the remaining residues. The model was drawn by a Microvax III using a program written by S. J. Remington.

histidine residue C2 proton chemical shifts for the native protein, protein in 6 M deuteriourea, *N*-acetylhistidine amide, and *N*-acetylhistidine amide with urea were made by combining aliquots of stocks of two different pH values to produce a distribution of final pH values. Solution conditions were maintained at 3 mg/mL protein or 5 mM *N*-acetylhistidine amide in 10 mM phosphate buffer containing 100 mM KCl except at extremely basic pH where it was necessary to dilute the basic stock solution with more basic solution of identical ionic strength and chloride concentration. The pH of each sample was measured before and after acquisition of a ^1H NMR spectrum. The spectra were recorded with a General Electric GN500 spectrometer using a jump–return pulse sequence to suppress residual water. Measurements of pH agreed to within 0.05 unit before and after spectral acquisition.

Standard protic buffers were used, and pH values are meter readings uncorrected for any deuterium isotope effect. The resulting titration data were fit with a nonlinear least-squares fitting routine in which the observed chemical shifts as a function of hydrogen ion concentration were fit to three parameters. These parameters were the protonated chemical shift, the unprotonated chemical shift, and the acid dissociation constant. In some cases the data were fit with a phenomenological Hill treatment involving a fourth parameter, the Hill coefficient representing the apparent proton order for the unprotonated to protonated equilibrium.

The conditions used for ^{13}C NMR were similar to those of proton NMR except samples were 20 mg/mL in buffers containing 10% D_2O and a one-pulse experiment with WALTZ proton decoupling was used to observe the carbon nuclear magnetic resonance spectrum. Between 2000 and 22000 transients were recorded for each spectrum depending on the desired signal-to-noise and sample concentration.

Results

Asp70–His31 Salt Bridge. Here we describe a specific salt bridge formed between histidine residue 31 (His31) and aspartic acid residue 70 (Asp70) which accounts for the maximum in stability near pH 5 observed for T4 lysozyme and contributes 3–5 kcal/mol to the free energy of the folded state.

The environment of this salt bridge is shown in Figure 1 as a computer-derived CPK model generated from the refined coordinates (Weaver & Matthews, 1987) of T4 lysozyme deduced by X-ray crystallography. Red represents the atoms of Asp70, and green represents the atoms of His31, while all other carbon atoms are white, oxygen atoms are purple, and nitrogen atoms are blue. Hydrogen atoms are not shown. The bound waters around the salt bridge have been removed for clarity. The refined model shows that the Asp70 and His31 side chains are well ordered with low temperature coefficients. As can be seen, the salt bridge is surface accessible from one side and is placed against a rather rigid network of amino acid residues which begin to form the hydrophobic core of the molecule. The salt bridge lies at the base of a cleft on the surface of the protein that contains the active site.

Thermodynamic Studies of His31 and Asp70 Mutants. The experiments described here employ a variant of the wild-type T4 lysozyme in which the two cysteine residues at positions 54 and 96 have been replaced by threonine and alanine, respectively. We refer to this doubly substituted variant as "pseudo-wild-type" protein. The pseudo-wild-type protein, unlike the wild type, does not precipitate at elevated pH, and the full pH dependence of its stability can be examined.

Figure 2 shows the pH dependence of the midpoint of the unfolding transition, T_m, of the pseudo-wild-type protein as a function of pH. This is determined with circular dichroism to monitor the two-state reversible unfolding (Becktel & Schellman, 1987) of the protein as a function of pH. The protein shows a broad bell-shaped curve in its stability with a maximum in stability near pH 5 corresponding to a transition temperature of 65 °C. The melting temperature decreases to about 20 °C at pH 1 and 12. This pH dependence of stability is typical of many proteins.

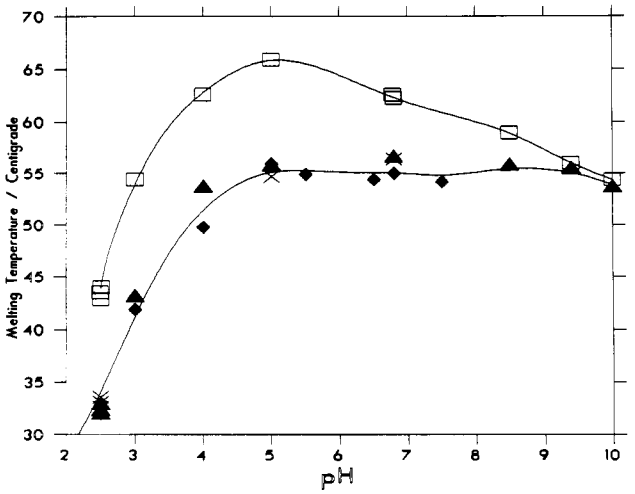

FIGURE 2: Plots of the midpoint of the reversible unfolding transition versus pH for thiol-free wild type (□), H31N (▲), D70N (◆), and H31N/D70N (×). Site-directed mutagenesis was performed with an M13 single-strand DNA containing a derivative of the T4 lysozyme gene in which codons for cysteine residues 54 and 97 had been changed to encode threonine and alanine, respectively [Matsumura et al. (1988) and references cited therein]. Denaturation of T4 lysozymes was monitored with the change in dichroism at 223 nm, as has been described (Becktel & Baase, 1987). The protein concentration was 0.02 mg/mL in buffers containing 10 mM potassium phosphate and 0.15 M KCl.

It is of interest that a decrease in stability is observed between pH 6 and pH 9. The protein contains only one histidine residue, and this is a prime candidate for a titratable group that might be involved in the pH-dependent change in stability near neutrality.

Using standard site-directed mutagenesis techniques (Zoeller & Smith, 1983), we constructed two single mutants of the pseudo-wild-type protein to eliminate the His31-Asp70 salt bridge. In one, the histidine residue at position 31 was replaced by asparagine (referred to as H31N), and in the second mutant, aspartic acid residue 70 was replaced by asparagine (referred to as D70N). We also constructed the double mutant (H31N/D70N). These mutations have little effect on the activity of the protein with H31N having 120%, D70N having 90%, and H31N/D70N having 90% the activity of the pseudo-wild-type protein.

Figure 2 also shows the pH dependence of the midpoint of the thermal unfolding transition for these mutants of the pseudo-wild-type protein. The introduction of either single mutation dramatically reduces the midpoint temperature, T_m, for the reversible unfolding equilibrium. Thus at pH 5.5 a net decrease of 11 °C in T_m is observed. The entropy of unfolding for the wild-type protein or thiol-free protein is about 360 eu at pH 5.5 (Matthews et al., 1987). Thus a change of 11 °C in T_m corresponds to a free energy change ($\Delta T\Delta S$; Becktel & Schellman, 1987) of about −4 kcal/mol in the unfolding equilibrium. In addition, the bell-shaped maximum in stability is removed, and the folding free energy of the mutants is essentially pH independent in the range pH 4.5–10.0. Breakage of the salt bridge by substitution of either the histidine or the aspartic acid residue of the salt bridge gives virtually identical stability versus pH curves; similarly, the double mutant H31N/D70N shows nearly the same stability curve as either single mutant in the pH range 2–7 as well as at higher pH values.

^1H and ^{13}C NMR Studies. To further characterize the interactions between His31 and Asp70, we employed nuclear magnetic resonance techniques to monitor the pK_a values of these residues in the native and mutant proteins.

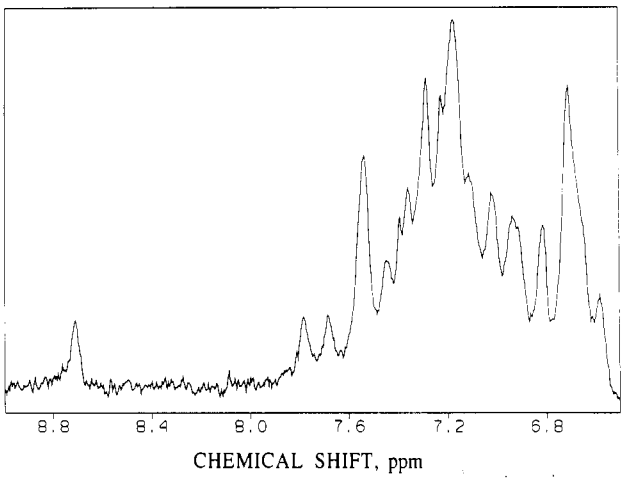

FIGURE 3: Downfield region of the proton magnetic resonance spectrum of thiol-free T4 lysozyme in 10 mM potassium phosphate buffer containing 0.1 M KCl, pH 5.95, at 10 °C in D_2O. The bulk of the amide protons was removed by heating the protein to 55 °C for 0.5 h in 10 mM D_3PO_4 and 10 mM KCl in D_2O. The resonance at 8.71 ppm is the C2 proton of His31.

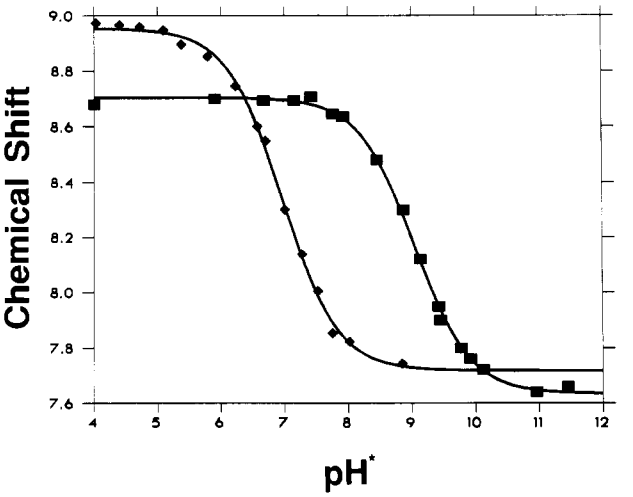

FIGURE 4: pH dependence of the chemical shift of the C2 proton of His31 in wild type (■) and D70N (◆). All titrations and pH measurements were performed at 10 °C with a pH meter uncorrected for deuterium isotope effects.

As shown in Figure 3, the single histidine C2 proton is easily observed by proton magnetic resonance. This resonance is lacking in the protein in which the histidine has been replaced by asparagine (data not shown). Figure 4 shows the pH dependence of the chemical shift of this resonance (squares). The shift is typical of that seen for the protonation–deprotonation equilibrium of histidine residues as a function of pH. The solid line shows the theoretical fit to a pK_a of 9.05 for a single titratable group without any cooperative interactions.

Figure 4 also shows the titration curve for the histidine C2 proton in the mutant D70N (diamonds). The pK_a value of the histidine in this mutant becomes 6.9, a more normal value. We have also estimated the unfolded pK_a of His31 in the unfolded protein by observing the shift of the C2 proton as a function of pH by using 6 M deuteriourea to unfold the protein. In 6 M urea and D_2O the apparent pK_a of His31 was observed to be 6.3, the pH meter reading uncorrected for D_2O or for urea being used. To estimate the effect of urea on the intrinsic pK_a and the glass electrode, we measured the apparent pK_a of *N*-acetylhistidine amide in H_2O alone and in 6 M urea in D_2O. This suggests a correction of 0.5 unit to account for the solvent effects on the pK_a and glass electrode. Using this

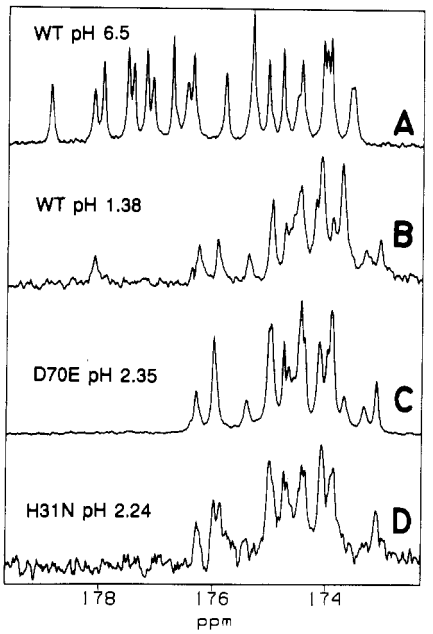

FIGURE 5: (A) ^{13}C magnetic resonance spectrum of the carbonyl region of [4-^{13}C]aspartate-(98%, MSD Isotopes) labeled T4 lysozyme using methods previously described. Protein concentration was about 1 mM in 90% H_2O/10% D_2O buffer containing 10 mM phosphate and 0.1 M KCl at 10 °C, pH 6.5. About 2000 transients were averaged to give spectra A–D. (B) ^{13}C magnetic resonance spectrum of the carbonyl region of the same sample as (A) but at pH 1.38 in 10 mM phosphate and 0.1 M KCl at 10 °C. (C) ^{13}C magnetic resonance spectrum of the carbonyl region of the mutant D70E labeled with [4-^{13}C]aspartate (98%) at pH 2.35 in 10 mM phosphate and 0.1 M KCl at 10 °C. (D) ^{13}C magnetic resonance spectrum of the carbonyl region of the mutant H31N labeled with [4-^{13}C]aspartate (98%) at pH 2.24 in 10 mM phosphate and 0.1 M KCl at 10 °C.

correction, we estimate the unfolded pK_a of His31 to be 6.8 in H_2O buffers of modest ionic strength; this is very similar to the value of 6.9 measured for His31 in the mutant H31N. This suggests few, if any, residues other than Asp70 interact with His31 to shift its pK_a. This result strongly suggests an electrostatic interaction between histidine 31 and aspartate 70 in which Asp70 is ionized at neutral pH and above. The presence of this charged residue shifts the pK_a of the histidine upward by about 2.3 units at 10 °C, corresponding to an interaction free energy of about 3.0 kcal/mol at 10 °C.

Figure 5 shows the carbonyl region of the ^{13}C NMR spectrum of T4 lysozyme in which [4-^{13}C]aspartate has been biosynthetically incorporated into the protein. In the host bacteria aspartate is readily converted into asparagine, and thus, both aspartate and asparagine carbonyl side chains are labeled and appear in the spectrum. This spectrum gives 21 lines at pH 6.50 corresponding to 10 aspartate and 12 asparagine residues with the resonance at 175.4 ppm corresponding to two carbonyl resonances. Side-chain carboxyl resonances shift to lower frequency (upfield) by about 3 ppm when protonated. Figure 5 also shows the spectrum obtained when the pH is adjusted to 1.38. All but one resonance of those observed above 176.5 ppm at pH 6.50 have shifted to frequencies lower than 176.5 ppm. The lone remaining resonance at 178.2 ppm corresponds to an aspartate residue since it is observed when the biosynthetic incorporation of aspartate is carried out in a host cell deficient in the conversion of aspartate to asparagine (data not shown). This resonance has a pH-independent chemical shift in the pH range 1.4–8.0. Figure 5C shows the spectrum obtained at pH 2.35 in the mutant D70E in which glutamic acid replaces Asp70. As can be seen, the resonance at 178.2 ppm is missing. There are small changes in the region to lower frequency that 176.5 ppm, which may reflect electrostatic or other structural perturbations. However, the order of the resonances and their approximate intensity are maintained. Thus the peak at 178.2 ppm corresponds to Asp70. The Asp70 resonance remains unshifted at pH 1.38 at the low extreme and at pH 8.0 at the high extreme. Thus, Asp70 does not appear to titrate over this range. Since Asp at position 70 as compared to asparagine results in a 2-unit upward shift of the pK_a of His 31, it is most likely that Asp70 is negatively charged above pH 8. Similarly, the ^{13}C shift supports the view that Asp70 is negatively charged at all pH values from 1.4 to 8.

Figure 5D shows the ^{13}C spectrum obtained when ^{13}C-labeled aspartic acid is incorporated in the mutant H31N. The spectrum was obtained at pH 2.24. The resonance at 178.2 ppm is missing, and now there are no low-field carboxyl resonances observed at low pH. Because of the much lower stability of this mutant, it is difficult to obtain sufficient material to generate the excellent signal to noise needed to assign and titrate all these resonances. However, it is clear that Asp70 has an approximately normal pK_a in the mutant H31N. Thus Asp70 has a much lowered apparent pK_a due to its interaction with His31.

We can set an upper bound on the value of the Asp70 pK_a in the wild-type protein of about 0.5 in the presence of protonated His31. Replacement of His31 by asparagine brings the Asp70 pK_a into the normal range. We can place a lower bound on its pK_a of 3.5–4.5 in this mutant. The proximity of this value to the noninteracting value of 4.0 suggests only small effects on the pK_a of Asp70 from charged groups other than His31 at pH 4 and above.

The shift in apparent pK_a of Asp70 corresponds to a free energy change of 4–5 kcal/mol at 10 °C. The shift in apparent pK_a seems to be somewhat larger for Asp70 than for His31. If no other considerations were to intervene, one would expect the electrostatic interaction between two groups to result in identical stabilization of the ionized pair in the salt bridge relative to their neutral forms an therefore equal free energy changes in the observed pK_a values from their noninteracting values. The apparent discrepancy from this expectation is not large, but it seems real. There are several potential explanations for the discrepancy. Since we cannot directly measure the pK_a of one member of the salt bridge pair when the other is charge neutral, we must simulate this condition by mutation. If the substitution of asparagine for either Asp70 or His31 is a poor model for the charge-neutral form of those amino acids, our estimate of the pK_a shifts would be incorrect. Similarly, there may be structural changes associated with the mutational substitution which make the mutational model less valid at the quantitative level. Since the overall charge on the protein differs near the pK_a of His31 (pH 9) and Asp70 (pH 1), there may be ionizable groups with pK_a values between 4 and 2 which indirectly or directly interact with Asp70 to further lower its pK_a value beyond that due to the His31 interaction. Finally, there may be anion binding sites near the salt bridge which change with mutation. We are in the process of investigating these possibilities.

Discussion

It is instructive to consider how proton binding is coupled to the folded–unfolded equilibrium. Here there are *m* binding sites for protons (H) on both the folded and unfolded protein:

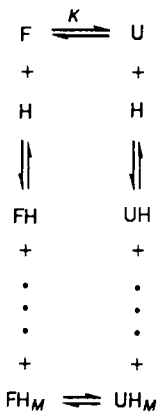

If F and U represent the unprotonated forms of the folded and unfolded proteins and the equilibrium between the unprotonated forms of F and U is characterized by an equilibrium constant K, then one can define an apparent equilibrium at any pH by

$$K_{app} = \frac{\sum_{i=0}^{m} UH_i}{\sum_{i=0}^{m} FH_i} = K \frac{1 + \sum_{i=0}^{m} \varphi_{ui} H^i}{1 + \sum_{i=0}^{m} \varphi_{fi} H^i}$$

(Wyman, 1964; Dahlquist, 1978) where φ_{ui} and φ_{ni} represent the phenomenological overall constants describing the binding of i protons to the unfolded and folded forms of the protein, respectively. Formally, the pH dependence of the unfolding equilibrium arises from the different values of the proton binding polynomials in the folded and unfolded states at various proton concentrations.

If we assume that the Asp70–His31 salt bridge pair is essentially thermodynamically isolated from all other ionizable groups in both the folded and unfolded states, the effects of only these two groups can be considered in isolation, and the scheme reduces to two protonation steps:

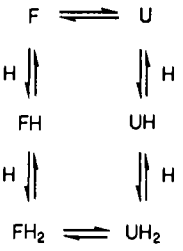

The first steps represents the protonation of His31 (folded pK_a = 9.05; unfolded pK_a = 6.7), and the second step represents the protonation of Asp70 (folded pK_a = 0.5; unfolded pK_a = 4.0). Figure 6 shows a plot of the variation in the free energy of folding (calculated as $-RT \ln K_{app}$) plotted as a function of pH by use of the pK_a values cited above. As can be seen, this gives a bell-shaped curve with a maximum difference in stability of about 5 kcal/mol at about pH 5 as compared to acid pH.

The maximum contribution of the salt bridge to the stability of the folded state is near pH 5.0. At this pH, Asp70 is negatively charged and His31 is positively charged in both the folded and unfolded states. As the pH is raised above pH 6.5, the contribution of the salt bridge to the stability of the folded

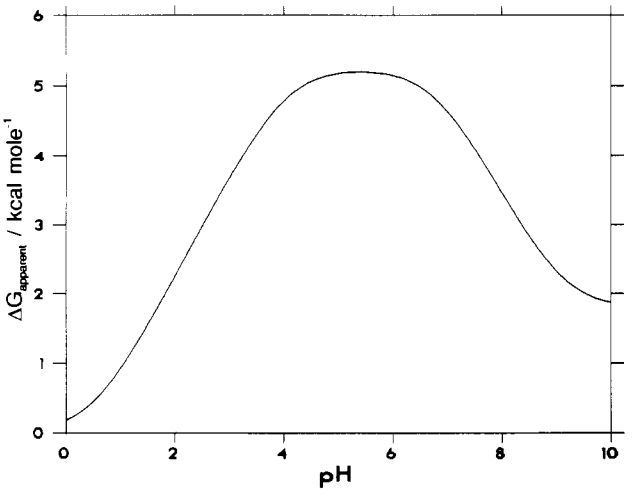

FIGURE 6: Plot of $-\Delta G_{app}$ as defined in the text versus pH at 10 °C. This theoretical curve is derived with the folded pK_a values of 0.5 and 9.05 and the unfolded pK_a values of 4.0 and 6.8 for Asp70 and His31, respectively.

state decreases as His31 becomes deprotonated in the unfolded state. This decrease continues as the pH is raised until (at pH 8) His31 starts to become deprotonated in the folded state. By pH 10, His31 is deprotonated in both the folded and unfolded states, and the contribution of His31 to the stability is constant above pH 10. The overall contribution of the protonation of His31 is about 3 kcal/mol, which stabilizes the folded state. The shift in pK_a value from 6.8 to 9.1 in the unfolded and folded states reflects this contribution to the overall free energy of the folded state. The pH dependence shown in Figure 6 reflects both the folded and unfolded pK_a values of His31. Similarly, the contribution of His31 and Asp70 to the overall folding free energy decreases as the pH is lowered below pH 5. The decrease begins near pH 4, corresponding to the protonation of Asp70 in the unfolded state, and continues as pH is lowered until the pH drops below 0.5, where Asp70 is protonated in the folded state. The overall contribution of the deprotonation of Asp70 to the folding equilibrium is about 5 kcal/mol, reflecting the change in pK_a value from 0.5 in the folded state is to 4.0 in the unfolded state. The energetics of Asp70 protonation differ from those of His31 and may reflect additional electrostatic interactions of Asp70 with the very positively charged protein at low pH.

The data shown in Figure 6 give qualitative agreement to the change in folding, and the free energy is estimated by the data shown from the thermal unfolding of wild-type and mutant proteins shown in Figure 2. The difference in thermal stability of 4 kcal/mol at pH 5 is calculated at about 50 °C with the unfolding data, and the pK_a shifts are measured at 10 °C so the data are not strictly comparable. However, the shifts in pK_a of Asp70 and His31 do not appear to be very temperature dependent, so we expect similar effects at 50 °C on the folding equilibrium. There is also a significant change in the heat capacity change due to unfolding in the pseudo-wild-type protein as compared to any of the mutants in which the salt bridge is broken. This further complicates comparison of the protein stabilities at temperatures much different from their respective T_m values.

Implications of the Coupling of pK_a's to Folding Equilibria. These results demonstrate that the folded form of the zwitterion of the salt bridge is more stable than either the fully protonated or deprotonated salt bridge. In addition, the double mutant D70N/H31N, which is charge neutral, is no more stable than either single mutant in which unmatched charges are produced above pH 4 (D70N) or below pH 7 (H31N).

This demonstrates that there is a specific interaction between His31 and Asp70 as opposed to a nonspecific additive effect of isolated charges. Thus, the zwitterionic salt bridge actively stabilizes the protein rather than minimizing the potential instability caused by the unmatched charges associated with either the fully protonated or fully deprotonated forms of the salt bridge.

The thermodynamic coupling of ionization constants and folding equilibrium in protein suggests a simple rule for evaluating the effects of ionizable groups on stability. If the native state stabilizes an interaction such as the His31–Asp70 salt bridge, the salt bridge correspondingly stabilizes the native state. Thus, detailed analyses of the apparent pK_a values of protein residues provide unique insight into the electrostatic forces stabilizing the folded state since these values directly probe the electrostatic contribution of each group to the overall protein stability. The further a pK_a value is lowered relative to its value in the unfolded state, the more the conjugate base stabilizes the folded structure. Conversely, the more the pK_a of an ionizable group is raised, the more the conjugate acid stabilizes the folded form as compared to the unfolded form. Our data suggest that Asp70 is a strong acid. Hence, the decreased stability observed a low pH does not result from protonation of the salt bridge. Rather, it arises from protonation of the unfolded state. As the pH is lowered below the unfolded pK_a of 4, the unfolded state is further stabilized as Asp70 protonates. This stabilization of the unfolded state continues as the pH is lowered until the acid concentration is sufficiently high to begin protonating Asp70 in the folded state (presumably beginning about pH 1.0), and finally, further increases in acid do not lower the stability of the folded state once Asp70 is essentially fully protonated. This view is qualitatively different from that originally proposed by Linderström-Lang in which the decrease in stability is due to protonating the folded state in a global fashion. Further investigations are needed to evaluate which model is more generally correct.

The pH dependence of T_m observed after the His31–Asp70 salt bridge has been removed by mutation shows that other acidic residues have perturbed pK_a's in the folded state. These appear to account for about an additional 8 kcal of stabilization and correspond to at least two aspartate or glutamate residues. We are in the process of identifying these residues and quantitating their contribution to the free energy of stabilization of the folded state.

In addition to the charge–charge interactions described here, it is becoming clear that charge–dipole interactions may also be of general importance in the energetics of protein folding (Nicholson et al., 1988). The data presented here suggest that certain salt bridge interactions may well be more important than had previously been generally accepted [see Shutz and Schirmer (1979) and Brown et al. (1978)]. Fersht (1972) described a salt bridge with an interaction energy of 3 kcal/mol in γ-chymotrypsin. It is possible that most proteins contain one or more of these more energetic salt bridges. Indeed since many proteins will unfold at low pH at room temperature or lower, interactions between ionizable groups may well account for the net stabilization energy favoring folding in globular proteins. Thus there are likely to be interactions of ionizable groups in most proteins which contribute to the stability of the folded state, and these contributions can be measured with the approach described here.

Registry No. Asp, 56-84-8; His, 71-00-1; lysozyme, 9001-63-2.

References

Becktel, W. J., & Baase, W. A. (1987) *Biopolymers 26*, 619–623.

Becktel, W. J., & Schellman, J. A. (1987) *Biopolymers 26*, 1859–1877.

Brown, L. R., DeMarco, A., Richarz, R., Wagner, G., & Wuthrich, K. (1978) *Eur. J. Biochem. 88*, 87–95.

Dahlquist, F. W. (1978) *Methods Enzymol. 48*, 270–299.

Elwell, M., & Schellman, J. A. (1977) *Biochim. Biophys. Acta 494*, 367–383.

Fersht, A. (1972) *J. Mol. Biol. 64*, 497–509.

Hawkes, R., Gutter, M. G., & Schellman, J. (1984) *J. Mol. Biol. 175*, 195–212.

Kunkel, T. A. (1985) *Proc. Natl. Acad. Sci. U.S.A. 82*, 488–492.

Linderström-Lang, C. R. (1924) *C. R. Trav. Lab. Carlsberg*, 15–70.

Matsumura, M., Becktel, W. J., & Matthews, B. M. (1988) *Nature 334*, 406–410.

Matthew, J. B., & Gurd, F. R. N. (1986) *Methods Enzymol. 130*, 413–453.

Matthews, B. W., & Remington, S. J. (1974) *Proc. Natl. Acad. Sci. U.S.A. 71*, 4178–4182.

Matthews, B. W., Nicholson, H., & Becktel, W. J. (1987) *Proc. Natl. Acad. Sci. U.S.A. 84*, 6663–6667.

McIntosh, L. P., Dahlquist, F. W., & Redfield, A. G. (1987a) *J. Biomol. Struct. Dyn. 5*, 21–34.

McIntosh, L. P., Griffey, R. H., Muchmore, D. C., Nielson, C. P., Redfield, A. G., & Dahlquist, F. W. (1987b) *Proc. Natl. Acad. Sci. U.S.A. 84*, 1244–1248.

Muchmore, D. C., McIntosh, L. P., Russell, C. B., Anderson, D. E., & Dahlquist, F. W. (1989) *Methods Enzymol. 177*, 44–73.

Nicholson, H., Becktel, W. J., & Matthews, B. W. (1988) *Nature 336*, 651–656.

Plateau, P., & Gueron, M. (1982) *J. Am. Chem. Soc. 104*, 7310–7311.

Sanger, F., Nicklen, S., & Coulson, A. R. (1977) *Proc. Natl. Acad. Sci. U.S.A. 74*, 5463–5467.

Schulz, G. E., & Schirmer, R. H. (1979) *Principles of Protein Structure*, Chapter 3, Springer-Verlag, New York.

Tanford, C. (1961) in *Physical Chemistry of Macromolecules*, Chapter 8, Wiley, New York.

Weaver, L. H., & Matthews, B. W. (1987) *J. Mol. Biol. 193*, 189–199.

Wyman, J. (1964) *Adv. Protein Chem. 19*, 223–286.

Zoller, M. J., & Smith, M. (1983) *Methods Enzymol. 100*, 468–500.